DOI: 10.13009/EUCASS2019-380

Experimental and Computational Analysis of Single Crystal Piezoelectrical Driven Synthetic Jet Actuator

Baris Gungordu, Mark Jabbal and Atanas Popov
Faculty of Engineering, University of Nottingham
NG7 2RD, Nottingham, United Kingdom
baris.gungordu@nottingham.ac.uk, mark.jabbal@nottingham.ac.uk, atanas.popov@nottingham.ac.uk

Abstract

This study aims to examine the velocity and efficiency improvement of a synthetic jet actuator by utilizing a single-crystal piezoelectric disc. Laser vibrometer and hot-wire anemometry were used in the experiments to measure diaphragm displacement and output velocity, respectively. Experiments achieved a peak electro-fluidic power conversion efficiency of 43% with a peak output jet velocity of 114 m/s. A multi-physics computational simulation was developed to reproduce the experimental results. The simulation results showed an acceptable match with experimental data. Peak displacement and peak output jet velocity matched with 5% and 3% with experimental data, respectively.

1. Introduction

According to the International Air Transport Association (IATA), the total number of passengers for commercial flights were 3.8 billion in 2016. The projected number of passengers is 7.2 billion in 2035. Currently, air transport accounts for 2% of the total global man-made carbon emissions. Clearly, this should be reduced. Flow control has a great potential to help towards achieving the CO_2 reductions by controlling the flow separation to reduce the aerodynamic drag.

Synthetic jet actuator displaces still air in the cavity by employing an actuation mechanism such as a piston, loudspeaker or piezoelectric diaphragm. The still air in the cavity gains momentum and discharges through the orifice. During discharge, the air in the cavity rolls-up and creates vortices with the interaction of the orifice edges. This gives a rise of an unsteady jet which is a train of discrete vortical structures [1].

Figure 1 illustrates a typical (i.e. horizontal diaphragm) SJA geometry with the formed vortex rings. SJA is characterized by the formation of vortex rings, which results in an unsteady jet. The oscillating diaphragm is usually a combination of the substrate material with a piezoceramic patch.

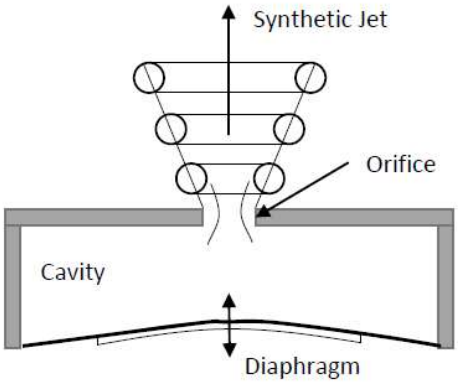

Figure 1: Cross-section of a horizontal-diaphragm SJA Geometry

Synthetic jet actuators have certain advantages for the full-scale implementation as a new generation active flow control device. They are compact in size (O ~ 10^{-6} m^3) and self-containing with no requirement for piping. Even though further

DOI: 10.13009/EUCASS2019-380

research is required, they can potentially achieve high enough jet velocity to have full-scale application in the aerospace industry. For a full-scale application, the output jet velocity should be at least 200 ms^{-1}.

The studies for design optimization of piezoelectrical-driven SJA are very numerous. Ugrina and Flatau [2] experimentally studied different diaphragm, orifice and cavity size. They identified the importance of sizing the actuator in a way that Helmholtz and disc's mechanical resonance should be close to each other. Feero et al. [3] studied different shapes of the cavity and identified the cylindrical cavity to have the maximum momentum flux.
Gomes and Crowther [4] proposed optimum dimensions of PZT-diaphragm, cavity and orifice for the maximum jet velocity. They carried various experiments with PZT-5A SJA with different cavity height. The study identified an optimum size of the actuator and the work resulted in a peak jet velocity of 130 ms^{-1} at 110V with an electro-fluidic efficiency of 7%. Currently, this work is the highest velocity achieved by an SJA with horizontal-diaphragm configuration (Figure 1).
The current state-of-art velocity is reported by Van Buren et al. [5]. They achieved an output jet velocity of 211 ms^{-1} with an adjacent diaphragm-orifice piezoelectrical driven SJA. Their efficiency for that velocity is reported to be 3.5%.

Lin et al. [6] implemented an array of SJA with PZT diaphragm on a small-scale vertical tail model. They achieved 20% side force enhancement at moderate rudder deflections. For large rudder angles, synthetic jet's momentum coefficient is not found enough, therefore, it is not applied in full-scale aircraft tests on a Boeing 757. Instead, they used 31-sweeping jet actuators to benefit their higher momentum and effectiveness in large rudder deflections. Hence, SJA requires further research before the full-scale application and to be able to grant effective control.

The efficiency of SJA is not very thoroughly investigated in the literature. Studies including [2], [3], [4], [5] concentrated on explaining the physics and achieving high jet velocity. Improving efficiency while having high jet velocity requires a comprehensive understanding of the losses of SJA. Poly-crystal (i.e. PZT-5A) diaphragm has a large electromechanical conversion loss, which account for nearly 60% of the total losses of SJA [7]. Consequently, to reduce the electromechanical conversion loss, single-crystal disc (PMN-PT) is proposed with this study. PMN-PT`s electromechanical coupling factor is 0.9 which is more than twice when compared with PZT-5A.

In order to achieve efficient flow control in aerospace applications, the actuator should be experimented in quiescent conditions to test their velocity output and efficiency. Jabbal et al. [8] studied PMN-PT SJA at a peak driving voltage of 20 V and achieved an efficiency of %47 with 40 ms^{-1}. It is an open question whether such a high efficiency could be attained at a higher driving voltage.

This study aims to compare PZT-5A and PMN-PT driven SJA`s electric-to-fluidic power efficiency to clarify the effect of enhanced electromechanical coupling factor of PMN-PT diaphragm at a higher driving voltage. The displacement profile of the PZT 5A and PMN-PT SJAs is measured using laser vibrometer. Hot-wire anemometry is used to acquire velocity output. Voltage and current signals are also recorded to lead the calculation of the electric-to-fluidic power efficiency. A computational model is developed to estimate the displacement profile and velocity output of the model.

After this section, methodology and a brief theory behind this study are presented. It is followed by experimental and computational approach sections. Then, the presentation of the results and discussions are presented. Finally, the conclusions are given.

2. Methodology and Theory

Within the scope of this paper, a fixed geometry SJA with PZT-5A and PMN-PT discs of the same size are experimentally and computationally studied.

SJA's efficiency (η) is expressed in terms of fluidic power it delivers and the electrical power it consumes.

Efficiency of an SJA is expressed by the Eq. (1).

$$\eta = \frac{\dot{F}}{\dot{E}} = \frac{output\ fluidic\ power}{input\ electrical\ power} \quad (1)$$

The output fluidic power expressed in terms of the mean peak jet velocity (U_{peak}), area of the orifice (A) and the air density (ρ) and it expressed with Eq. (2).

$$\dot{F} = \frac{1}{2}\rho A \, U_{peak}^{3} \quad (2)$$

The power has calculated by multiplication of current and voltage while accounting for the phase difference between current and voltage signals due to the electrical capacitance of the diaphragm [8].
Size of the disc, cavity and orifice are identical to the study by Gomes and Crowther [4]. Table 1 below demonstrates the common dimensions of the PZT-5A and PMN-PT discs.

Table 1: Dimensions of PZT-diaphragm

	Brass diameter (mm)	**PZT-patch diameter (mm)**	**Brass thickness (mm)**	**PZT-patch thickness (mm)**
Diaphragm Dimension	27	19.8	0.22	0.23

Figure 2 shows a 3-D illustration of the SJA used in the experiments and simulations.

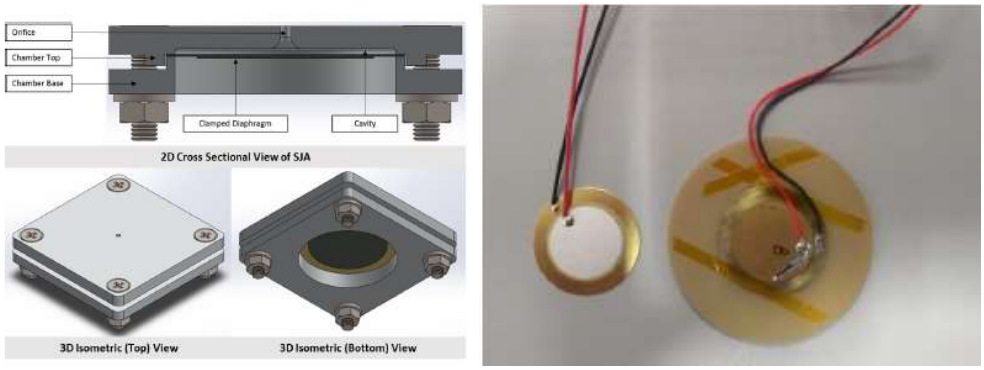

Figure 2: 3-D Illustration of the actuator, PZT-5A and PMN-PT (right, on a protective base) [8]

Both discs are <001> poled to give maximum displacement in the vertical to displace more air volume through the orifice. The physical properties associated with the electromechanical conversion are listed in Table 2 for PZT-5A and PMN-PT.

Table 2: Electro-mechanical properties of PZT-5A and PMN-PT

	PZT-5A	**PMN-PT**
D_{33} (pm/V)	300	1900
K_p (-)	0.4	0.9

The velocity response of an SJA characterized by two peaks which are associated with two resonant frequency. Those are the Helmholtz and diaphragm's mechanical resonance which are acoustical and mechanical phenomenon respectively.

PMN-PT disc has a maximum permissible peak voltage of 45 V based on its electric field of 2.0 kV/cm and thickness of 0.23 mm. Therefore, the peak voltage is selected as 40 V which is close to its maximum voltage and to avoid fracture.

DOI: 10.13009/EUCASS2019-380

3. Experimental Approach

The diaphragm excitation is made between 100-4000 Hz with intervals of 100 Hz at 40 V_p. For the experimental study, four different measurements are taken for each set of voltage including centre disc displacement, output jet velocity, the voltage applied and current drawn for each frequency of forcing.

The measurements are taken with laser vibrometer (PSV-200), hot-wire-anemometry (probe Dantec 55P11), signal generator/analyser (SR785) and two digital multi-meters. The laser vibrometer was connected to the signal generator which sent a sinusoidal signal through the Trek PZT350A high-voltage piezo amplifier to drive the diaphragm. The laser targeted to the centre of the disc and various readings are taken. The amplitude error of the laser equipment is ± 1.5%. The raw data is acquired in mm/s/V and converted into displacement in post-processing using MATLAB.

For the hot-wire-anemometry measurements, piezo amplifier is controlled by a TTI TG215 2MHz function generator. The function generator tuned to send sinusoidal voltage waveforms in the selected frequency. Figure 3 introduces the test rig, hotwire probe and vibrometer. The piezoelectric disc is fully clamped to have a net 25 mm diameter of disc. The voltage applied to the disc is monitored throughout the experiments and necessary adjustments made to ensure adequate voltage amplitude for all excitation frequency.

Calibration of hot wire anemometry is made using an in-house nozzle. HWA results are captured using a 1-D probe at a sampling frequency of 20,000 Hz. The number of samples for each actuation frequency is 200,000.

The probe is positioned to the centre of the orifice at a vertical distance of 1 orifice diameter. The acquired voltage is post-processed to fit King's Law. The percentage error in the velocity measurement using hot-wire anemometry is ± 3%.

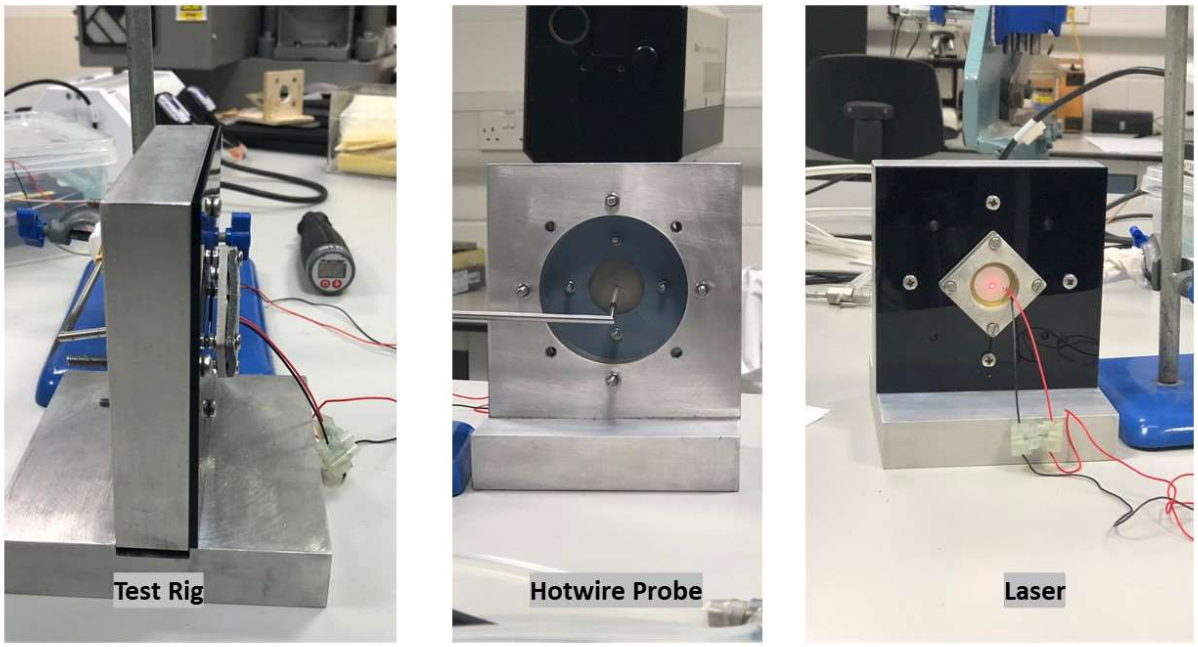

Figure 3: Experimental set-up

DOI: 10.13009/EUCASS2019-380

4. Computational Approach

A multi-physics computational simulation is developed for PZT-diaphragm and velocity modelling of SJA. COMSOL Multi-physics (version 5.3a) [9] is utilized. The computational model has a 2-D axisymmetric geometry to reduce computational time. The geometry is presented in Figure 4. It, also, presents the boundary conditions of the simulation.

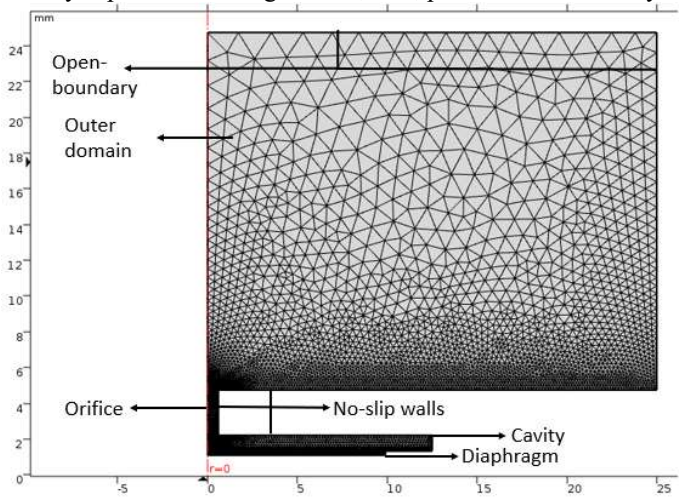

Figure 4: Simulation Geometry with main components of SJA & Boundary Conditions

Within the scope of the computational work, PZT-disc`s displacement profile, jet velocity output and current drawn by the disc are computed. The computations are conducted separately for PZT-5A and PMN-PT disc.

The physics behind the piezoelectrical-driven actuator is modelled using four different physical domains. These four domains include solid mechanics for PZT-diaphragm characteristics, electrostatics for AC Voltage which drives the disc, pressure acoustics to capture Helmholtz resonance behaviour and thermo-viscous flow to capture velocity and losses of SJA. The listed physics are coupled to reflect the finest possible characteristics of a PZT-driven SJA.

Open boundaries are selected to represent the quiescent conditions. They also prevent the backscatter of the flow which may affect the flow field. The walls of the cavity and orifice are modelled as no-slip walls.
The mesh shape and size have a significance in computational fluid dynamics type simulations. The mesh elements have tetrahedral and triangular shapes. The largest mesh element in the cavity and orifice are set to 0.15 mm. The mesh density is reduced in the outer domain to reduce the computational cost of the simulation. The mesh convergence test conducted to ensure results are mesh independent.

5. Results and Discussion

To serve for the best fit within the scope of this conference proceeding paper only the selected experimental and computational results are comparatively presented. The experimental results of diaphragm displacement and peak jet velocity output are compared with the numerical model developed.

5.1 PZT-5A : Displacement and Velocity

In Figure 5, the displacement profile for PZT-5A is presented. Experimental and computational results are compared. The peak frequency coincides at 2900 Hz at both studies which is the mechanical resonance of the PZT-diaphragm. Experimental and computational peak-to-peak displacement has found as 31 μm and 30 μm, respectively.

DOI: 10.13009/EUCASS2019-380

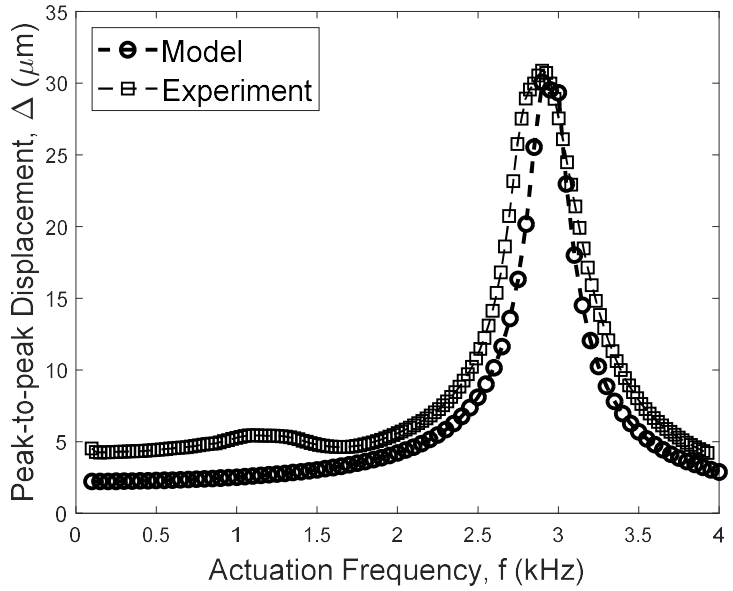

Figure 5: PZT-5A Experimental and computational diaphragm displacement profile – 40V_p

In Figure 6, the mean peak jet velocity versus the frequency is presented for PZT-5A for the peak voltage of 40V. As expected, there are two peaks which are associated with the Helmholtz and mechanical resonance. The mechanical resonance is at 2900 Hz which is also captured with the laser vibrometer scanning.

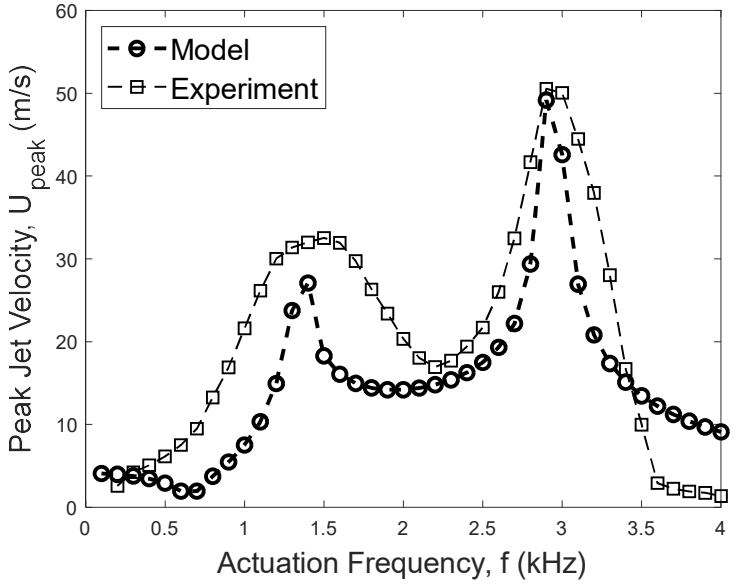

Figure 6: Mean peak jet velocity versus actuation frequency for 40 V_p

Table 3 presents the mean peak jet velocity at the resonant frequencies.

Table 3 : Resonance peak jet velocity result for PZT-5A at 40V_p

	Helmholtz Resonance Velocity (ms^{-1})	**Mechanical Resonance Velocity (ms^{-1})**
Experimental	33	51
Computational	28	49

DOI: 10.13009/EUCASS2019-380

In experimental and computational studies, the peak velocity is at the resonant frequency of 2900 Hz. The model has predicted the peak velocity with acceptable accuracy for the diaphragm resonance frequency. There is 2 ms^{-1} shortfall of the model's peak velocity when compared with the experimental result.

On the other hand, experimental Helmholtz frequency is at 1500 Hz, which is predicted as 1400 Hz at the model. The model has a shortfall of 5 ms^{-1} in peak Helmholtz resonance velocity. The overall shape is accurately covered.

5.2 PMN-PT: Displacement and Velocity

In Figure 7, the displacement profile for PMN-PT is presented. This figure is also comparing experimental and computational results. The peak frequency is located at at 2800 Hz in both studies which corresponds to the mechanical resonance of the PZT-diaphragm. Experimental and computational peak-to-peak displacement has found as 31 μm and 30 μm, respectively.

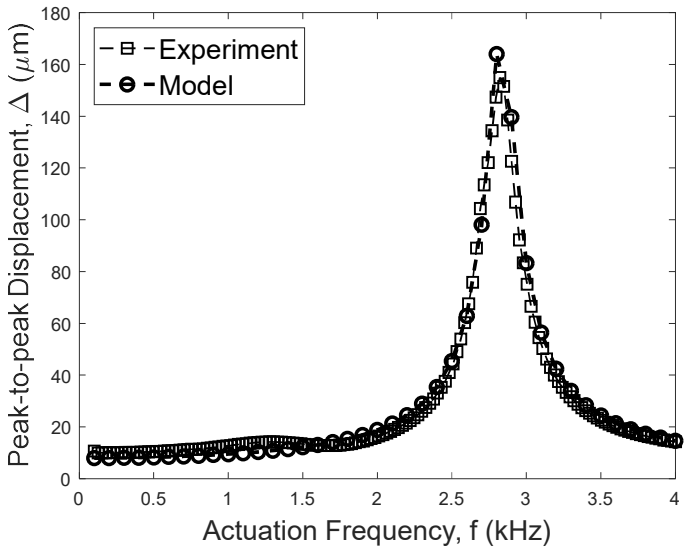

Figure 7: PMN-PT Experimental and computational diaphragm displacement profile – 40V_p

Figure 8 presents the mean peak jet velocity of the SJA with PMN-PT disc at 40 V_p.

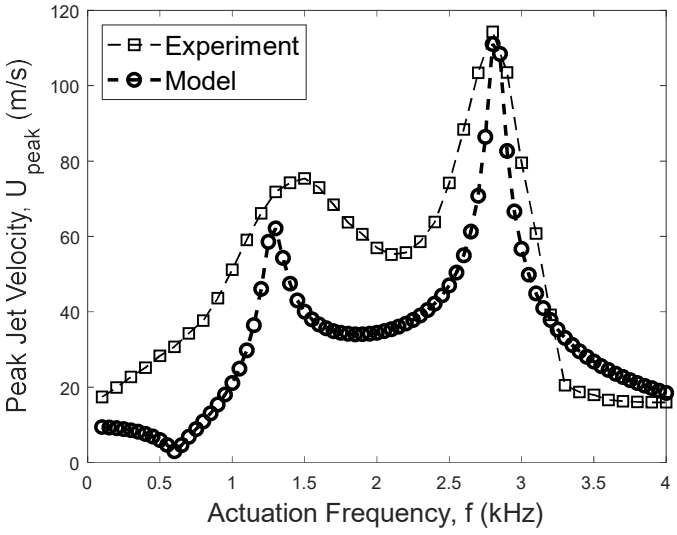

Figure 8: Mean peak jet velocity versus actuation frequency for 40 V_p

DOI: 10.13009/EUCASS2019-380

Table 4 presents the mean peak jet velocity at the resonant frequencies.

Table 4 : Resonance peak jet velocity results for PMN-PT at $40V_p$

	Helmholtz Resonance Velocity (ms^{-1})	**Mechanical Resonance Velocity (ms^{-1})**
Experimental	75	114
Computational	62	111

There is 3 ms^{-1} shortfall of the model's peak velocity when compared with the experimental result. The model has predicted the peak velocity with an acceptable accuracy for the diaphragm resonance frequency. Also, experimental Helmholtz frequency is at 1500 Hz, which is predicted as 1300 Hz at the model. The model has a shortfall of 13 ms^{-1} in Helmholtz resonance velocity. The overall shape is accurately covered to reflect occurrence of the double peaks.

5.3 Experimental SJA Efficiency

Figure 9 is presented to compare the efficiency of PZT-5A and PMN-PT SJAs at 40 V_p.

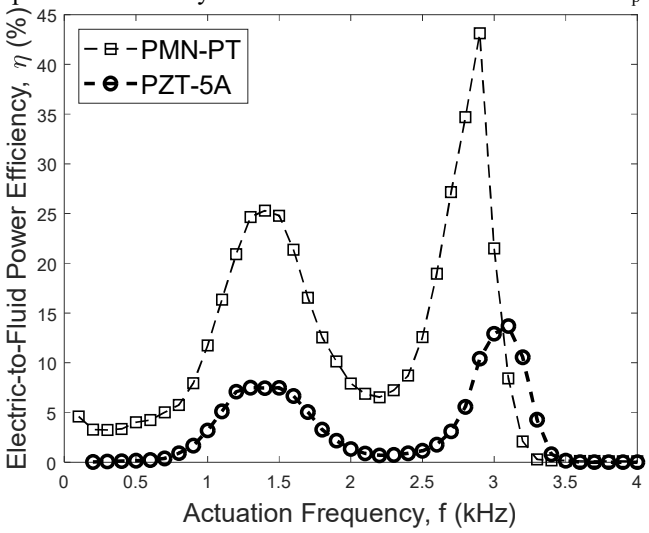

Figure 9: Experimental Electric-to-Fluid Power Efficiency Comparison of PZT-5A and PMN-PT

As seen Table 5, peak efficiency is shifted after the resonant frequency for both discs. PZT-5A shown a peak efficiency of 14% at 3.1 kHz for a velocity of 44.5 ms^{-1}.

Table 5 : Electric-to-Fluidic Power Efficiency (%)

	Peak Efficiency (%)	**Helmholtz Resonance Efficiency** (%)	**Mechanical Resonance Efficiency** (%)
PZT-5A	14	7	10
PMN-PT	43	25	35

Yet, for PMN-PT the peak efficiency is located at 2900 Hz with 43% at 103 ms^{-1}. Notably, PMN-PT has provided a 3-fold increase in peak efficiency.

5.4 Discussion

The results have revealed the highest efficiency published to-date for output jet velocity more than 100 ms^{-1} with 43%. Also, the mechanical resonance has the efficiency of 35% with an output velocity of 114 ms^{-1}. With a similar actuator geometry, Gomes and Crowther [4] have achieved 130 ms^{-1} with 7% of efficiency at 125 V_p. Table 6 reports the highest efficiency or velocities reported with their respective driving voltages and major components of actuator geometry d (orifice diameter) and D (cavity diameter).

Table 6 : Reported SJA efficiencies in the literature

	d (mm)	**D** (mm)	**Voltage** (V)	**Velocity** (ms^{-1})	η (%)
Gomes & Crowther (2006)	1.2	25	125	130	7
Li et al. (2011)	1 x 4	30	80	35	25
Feero et. al. (2015)	2	30.8	100	50	45
Girfoglio et al. (2015)	5	80	35	25	65
Van Buren et al. (2016)	1 x 12	80	150	120	3.5
Jabbal et al. (2018)	1.2	25	20	41	47
Present Study	1.2	25	40	114	35
Present Study	1.2	25	40	103	43

The shift in the peak efficiency is thought to be due to pole co-location and current draw characteristics of the disc. The pole co-location can be caused by the dielectric saturation of the PZT-patch.
The normalized current drawn is given in Figure 10. For both discs, the peak current is at 2800 Hz and it descends beyond that frequency before it increases again. The shift in the peak efficiency is due to this characteristic.

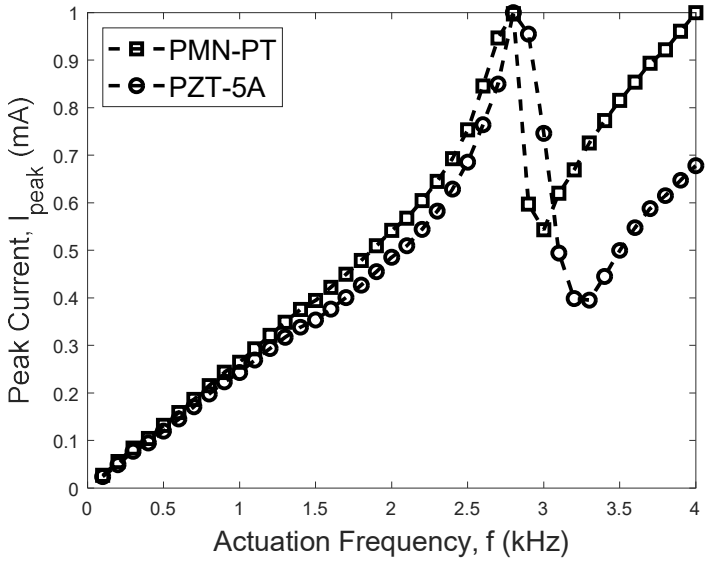

Figure 10: Normalized experimental current draw for PZT-5A and PMN-PT

DOI: 10.13009/EUCASS2019-380

The model developed is in 2-D axisymmetric geometry and designed to reflect the flow physics behind an SJA. It is first known numerical simulation which is employed to estimate relatively high velocity response. The physics behind the model includes the structural, acoustical, electrostatics, and fluid-dynamical elements. The model accounts for the suction period of SJA which equips it with an important advantage when compared to lumped element models (LEM). Also, it is capable to provide time-dependent visualisation of the flow structures.
The experimental resonant peaks are more spread in the frequency band wherein the model the peaks are less damped. The shortfall in some regions of the velocity output considered as the model's 2-D axisymmetric geometry and the way viscous losses are accounted.

The model had an acceptable diaphragm displacement and output jet velocity response covering both resonance frequency. Even though the Helmholtz resonance velocity is slightly smaller than the experimental values, the mechanical resonance is covered accurately both in terms of frequency and velocity.

6. Conclusions

An experimental and computational investigation were conducted to compare the single crystal PMN-PT discs with polycrystalline PZT-5A with the same dimensions on a fixed geometry actuator. Diaphragm displacement, velocity and efficiency of the SJA was significantly higher for PMN-PT SJA due to its enhanced electromechanical coupling coefficient.

Within the scope of experimental work, laser vibrometer and hot-wire anemometry was used for diaphragm displacement profile measurements and exit jet velocity respectively. Also, the voltage and current were recorded.
On the other hand, a new computational model was established, and simulations were carried out with the parameters and dimensions used in the experiments. The results have shown acceptable match with the experiments, especially at the resonant frequencies.
The conclusions of this study are as the following:

- At 40 V_p of diaphragm driving voltage, the PMN-PT SJA have 5 times more displacement than the PZT-5A SJA.
- PMN-PT SJA have 3 times more electric-to-fluidic power efficiency than PZT-5A SJA.
- Two discs have a difference of 100 Hz in their resonant frequency due to different material properties. This cause a change in the Helmholtz frequency as well.
- Numerical simulation has accurately estimated the displacement profile and resonant peak velocity and their associated frequency of the SJA.
- Peak displacement and peak output jet velocity matched with 5% and 3% with experimental data, respectively.

References

[1] Glezer A., Amitay A., "Synthetic Jets", 2002, Annual Review of Fluid Mechanics, 34:503-29
[2] Ugrina S., Flatau A.B., 2004, Investigation of synthetic jet actuator design parameters. In: Flatau AB (ed) Smart Materials and Structures, vol 5390, p 284. https ://doi.org/10.1117/12.54754 1
[3] Feero M.A., Lavoie P., Sullivan P.E., 2015, Influence of cavity shape on synthetic jet performance. Sensors & Actuators : A Physical 223:1–10. https ://doi.org/10.1016/j.sna.2014.12.004
[4] Gomes L. and Crowther W., 2006, "Towards a practical piezoceramic diaphragm based synthetic jet actuator for high subsonic application – effect of chamber and orifice depth on actuator peak velocity", 3rd AIAA Flow Control Conference, Fluid Dynamics and Co-located Conferences, doi:10.2514/6.2006-2859
[5] Van Buren T., Whalen E., Amitay M., 2016, "Achieving High-Speed and Momentum Synthetic Jet Actuator", Journal of Aerospace Engineering, Volume 29-2.
[6] Lin J.C., Andino M.Y., Alexander M.G., Whalen E.A., Spoor M. A., Tran J. T., Wygnanski I.J., 2016, "An Overview of Active Flow Control Enhanced Vertical Tail Technology Development", 54th AIAA Aerospace Sciences Meeting San Diego,California,USA doi:10.2514/6.2016-0056
[7] Jabbal M., 2009, "Flow Control Actuators for the 2020 Civil Transport Aircraft", AVERT Technical Report, [unpublished].
[8] Jabbal M, Dave R., Nesvijski E. N, "Efficiency enhancement of synthetic jet actuators using single crystal piezoceramics", 2018, In Proceedings of The Royal Aeronautical Society Applied Aerodynamics Conference, Bristol, UK, 23-26 July 2018.
[9] https://cdn.comsol.com/documentation/5.3.0.316/IntroductionToCOMSOLMultiphysics.pdf [Last Accessed: 14.06.2019]